DJS Vol. 46(3) (2023) –pp.144-158 ISSN: 1012-5965

Delta Journal of Science
Available online at
https://djs.journals.ekb.eg/

Research Article

GEOLOGY

Reservoir Characterization of the Jurassic Safa Formation, Shoushan Basin, North Western Desert, Egypt

Mai El-Ghandour[*1], Abdelmoneim Abu Shady[2], Abdelaziz Abdeldayem[1] and Ali Soliman[1]

[1]Geology Department, Faculty of Science, Tanta University, Tanta 31527, Egypt
[2] PetroNefertiti Petroleum Company, Zahret El Maadi Tower, Maadi, Cairo, Egypt.
Corresponding author: Mai El-Ghandour[1] **e-mail:** *Mahy_317@yahoo.com*
Received: 31/5/2023 **Accepted:** 11/7/2023

KEY WORDS

Reservoir, Safa Formation, Shoushan Basin

ABSTRACT

This study assesses the lithological and petrophysical properties of the Jurassic Safa reservoirs in western part of the Shoushan Basin, north Western Desert of Egypt. Composite logs from five wells from TUT and Salam fields were utilized to evaluate the different petrophysical parameters. Well log analysis, using Density/Neutron (D/N) dia-porosity cross-plots and tri-porosity (M-N) cross-plots, have been used to determine the lithology and porosity of the studied reservoirs. According to the results of litho-saturation cross-plots, the Lower Safa Member is primarily made up of sandstone, with a few interbeds of limestone, shale intercalation, and calcareous cement, while the Upper Safa Member is primarily made up of shale, with a few beds of limestone, sandstone bodies. The effect of natural gas appears in some D/N cross-plots in both Members. Petrophysical parameters derived from vertical litho-saturation cross-plots were used to identify each well's most effective sand zones. Movable hydrocarbon is found to increases mostly at northeastern and middle parts of the Lower Safa reservoir and at the southeastern and northeastern parts of the Upper Safa reservoir. Constructed iso-parametric maps of the Lower Safa reservoir display that the northeastern and northwestern parts of two studied fields is the most promising area for future development while that for the Upper Safa reservoir display that the south-eastern and northeastern parts of the studied fields are the most areas for future development.

Introduction

The Western Desert of Egypt still has a substantial hydrocarbon potential (**Dolson *et al.*, 2001; Eysa 2016**), with up to 90% of oil reserves and 80% of gas in the basins of the north Western Desert are not yet discovered with a complex geological structure composed mainly of a half-graben (**Zein El-Din *et al.*, 2001**). The study area is located in the Shoushan Basin **(Fig. 1)**, a large hydrocarbon province with significant Jurassic and Cretaceous oil and gas accumulations. It lies between latitudes 30° 40′ and 30° 47′ N and longitudes 26° 51′ and 27° 05′ E (**Fig. 1**). It has drawn the attention of many researchers and oil companies for its importance in hydrocarbon exploration.

There existing horst and half-graben structures in the north Western Desert are taking the form of parallel, elongated, tilted fault blocks with concomitant erosion of the upthrown blocks **(Shalaby *et al.*, 2013 and Abdel-Fattah, 2017) (Fig. 2).** Many authors (e.g., **Amin, 1961; Said 1962, El-khadragy and Sharaf, 1994; Shalaby *et al.*, 2000; Zein El-Din *et al.*, 2001; and El-khadragy *et al.*, 2010; Osman *et al.*, 2017; Abdel-Fattah *et al.*, 2019; El-Dakak *et al.*, 2021; Saad *et al.*, 2023; Badawy *et al.*, 2023**) have discussed the structural setting of the north Western Desert. The Shoushan Basin structures resulted from anticline features that were draped over or faulted due to vertical displacement of basement blocks (**Sultan and Abd El-Halim 1988**).

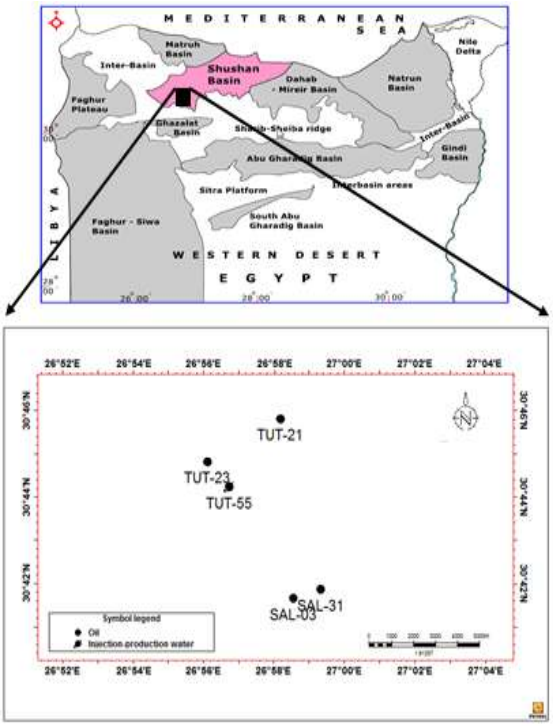

Fig. (1): Location map of the study area and distribution of the studied wells in study area

According to **Keeley *et al.*, (1990),** the Khatatba Formation comprises both the Zahra and Safa formations (**Fig. 3**). The Safa Formation is subdivided further into Lower and Upper members that the Kabrit Member separates, distinguished by the prevalence of limestones interbedded with claystone and sandstone **(EGPC 1998)**. The Lower Safa Member is consisted mainly of sandstone, siltstone, and coal with varying amounts of shales.

It is overlain by the carbonate – rich Kabrit Member and is underlain by the Paleozoic rocks **(EGPC, 1998)**. The Kabrit Member shows the effect of shale intervals and limestone as active seal rocks with very low permeability and porosity. The Upper Safa Member, on the other hand, overlies the Kabrit Member and underlies the Zahra Member, consisting of shales, siltstones, and sandstone with minor limestone. The age of the Upper Safa Member is Lower Bajocian - Early Bathonian **(Fig. 3**).

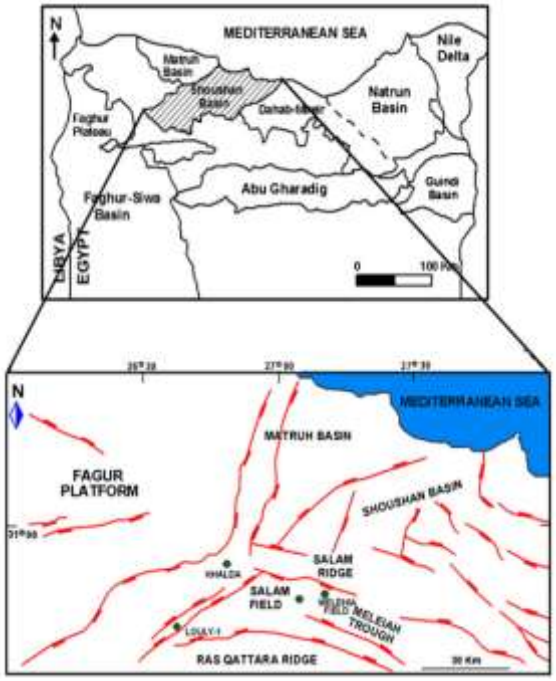

Fig. (2): Location map of the main Mesozoic basins in the Western Desert, showing the major Structural features and main faults in Shoushan Basin. **(EGPC 1992; Shalaby *et al*., 2013)**.

The applications of structural studies and their relation with hydrocarbon traps of the north Western Desert has been treated in several other publications (**e.g. Meshref 1982, Sultan and Abd El-Halim 1988, Abu Shady 1998, El Awady *et al*., 1998 and Shalaby *et al*., 2000**).

The main objectives of this study are to identify the different reservoir parameters characterizing the pay zones, determine the reservoir lithology and porosity using Density-Neutron and M-N cross-plots, and construct isoparametric maps from well log data to identify the most effective sand zones and highlight other promising locations for further exploration activity.

Materials and Methods

The study uses five wells from TUT and Salam fields; TUT-21, TUT-23, TUT-55, Salam-3X and Salam-31. The good logs of these five wells include Gamma ray (GR), Caliper log, Bulk Density (RHOB), Neutron porosity (NPHI), shallow, medium and deep later logs and micro spherical logs (ILS, ILM and ILD and MSFL), and Sonic log (DT). The lithology and porosity of the Lower and Upper Safa reservoirs were determined from logs using (Density/Neutron) cross-plots and tri-porosity (M-N) cross-plots.

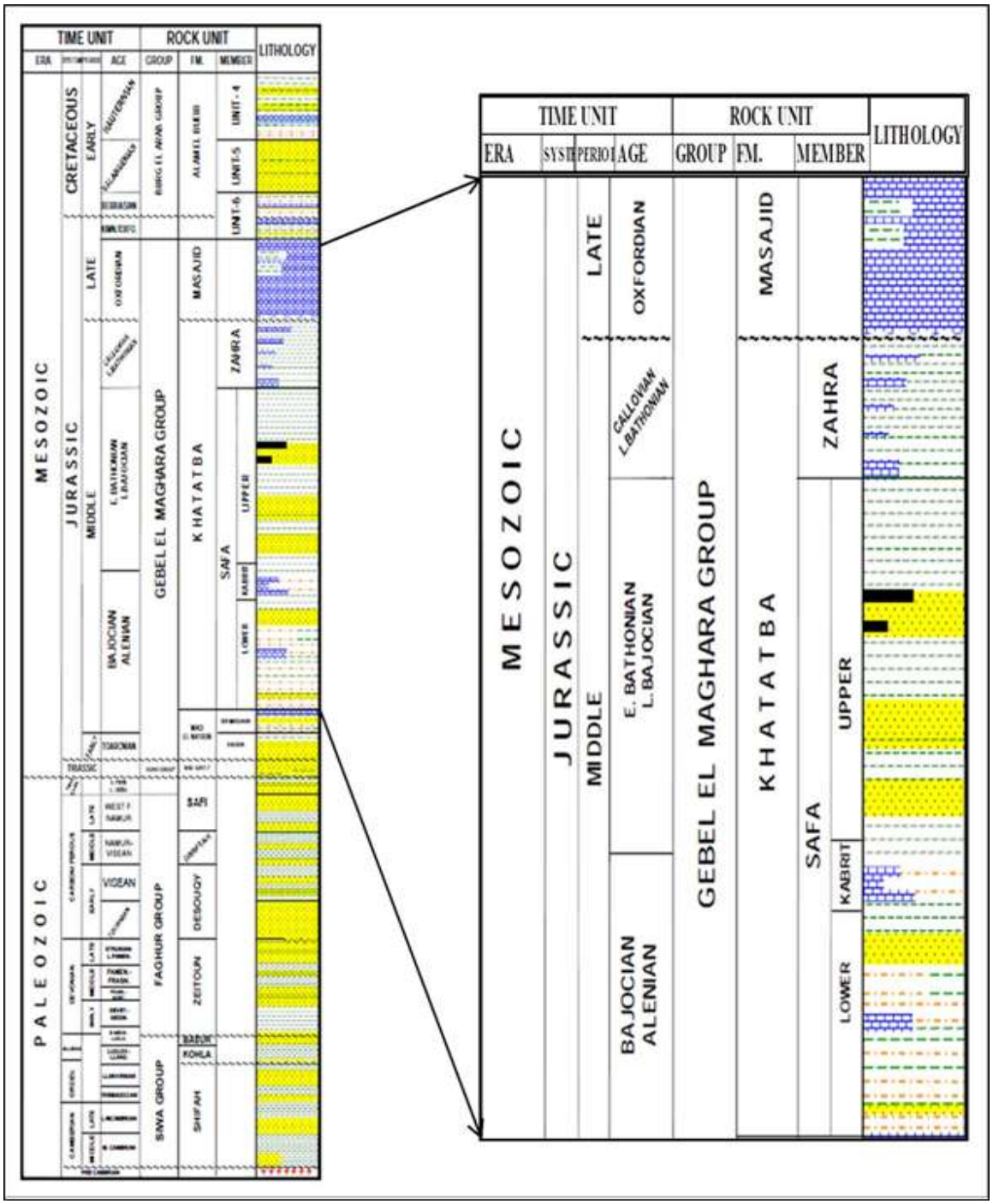

Fig. (3): Generalized stratigraphic column of northern Western Desert (**Khalda, 2010**).

The well log analysis software package Interactive Petrophysics V 3.5 (IP) was used to perform this complex integrative operation for formation evaluation and well log data analysis. The most effective sand zones of the Lower and Upper Safa reservoirs were identified in each well using vertical litho-saturation cross-plots of the petrophysical parameters that were taken from the well log data. These cross-plots are used to present the vertical distribution of the

lithology, fluid content and porosity. This analysis helps identify prospective hydrocarbon-bearing zones in the area. Additionally, distribution maps for gross thickness, gross sand, net pay thickness, net/gross, effective porosity, water saturation, shale volume, and hydrocarbon saturation are created using the findings of well-log analysis. The net pay thickness is calculated using 6% effective porosity (Φe), 35% for shale volume (Vsh) and 50% for water saturation (Sw) cut off values (Personal communication with Khalda Petroleum Company, 2020).

Results and Discussion

Lithology and Porosity Determination Using Density - Neutron Crossplots

Figure (4) shows the density-neutron cross-plots of the Jurassic Lower Safa reservoir for the investigated wells. It is noted that most of plotted points align mainly around sandstone line, with some points lying between the sandstone and limestone lines in TUT-21, TUT-23, TUT-55, and Salam-31 wells. This reveals that this reservoir is primarily made of sandstone and a small amount of calcareous cement. The porosity values range from 3% to 17%. The few scattered points around the dolomite line are attributed to dolomitic cement and shale effect at TUT-23 well **(Fig.4)**. Some points are moved upward over the sandstone line due to the gas's influence.

Figure (5) illustrates the density-neutron cross-plots of the Upper Safa reservoir for the studied wells. It can be seen that most of the plotted points are located around the sandstone line, with the remaining points located between the sandstone and limestone lines. This reveals that this reservoir is primarily made of sandstone and a small amount of calcareous cement. The porosity values range from 5% to 20%. Scattered points displayed around the dolomite line are attributed to presence of dolomitic cement. Gas's influence moves some points upward over the sandstone line.

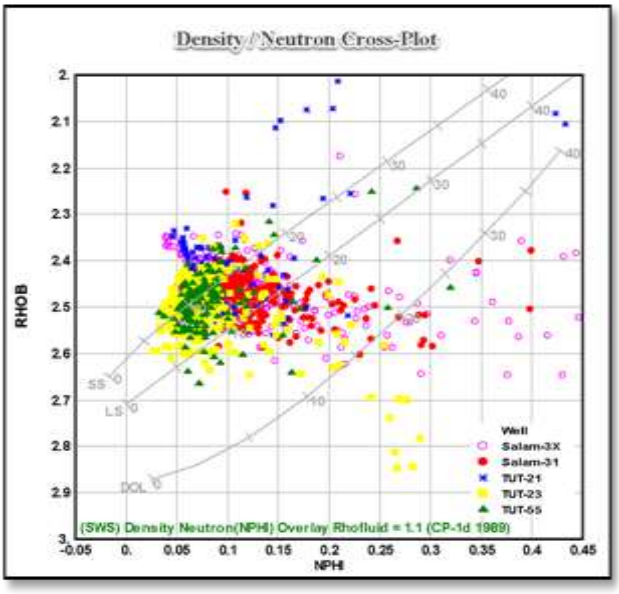

Fig. (4): Density - neutron cross-plots for the Lower Safa reservoir.

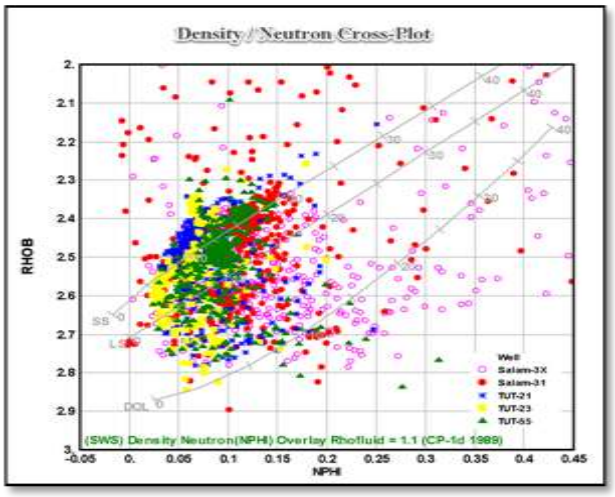

Fig. (5): Density - neutron cross-plots for Upper Safa reservoir

Determination of Lithology Using M-N Cross-plots

Figure (6) shows the mineralogical composition of the Lower Safa reservoir in the studied wells, except for TUT-55 well as M and N values could not be determined due to the absence of sonic log. Despite often being closer to the sandstone line, it is seen that the majority of plotted points are dispersed throughout the area between sandstone and limestone. The effect of gas is evident from the clear shift of some points to the upright corner of the diagram. In TUT-23 well, however, some points are moved downwards near the dolomite line indicating the occurrence of dolomitic cement **(Fig. 6)**.

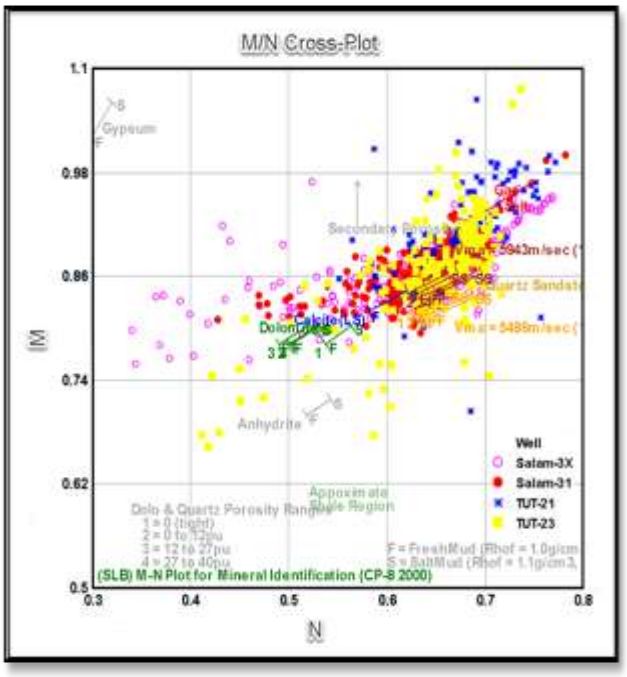

Fig. (6): M-N cross-plot for the Lower Safa Reservoir in TUT-21, TUT-23, Salam-3X and Salam-31wells.

Figure (7) shows the mineralogical composition of the Upper Safa reservoir in the wells under study, except for TUT-55 well. The majority of the plotted points are dispersed between the sandstone and limestone, although generally nearer to the sandstone line. The effect of the gas is evident from the clear shift of some scattered points from all wells to the upright corner of the diagram. However, some points are shifted downwards near the dolomite region, reflecting the presence of dolomitic cement and shale effect except in Salam-3X well. Points from some wells are also shifted upward probably due to secondary porosity effect **(Fig. 7)**.

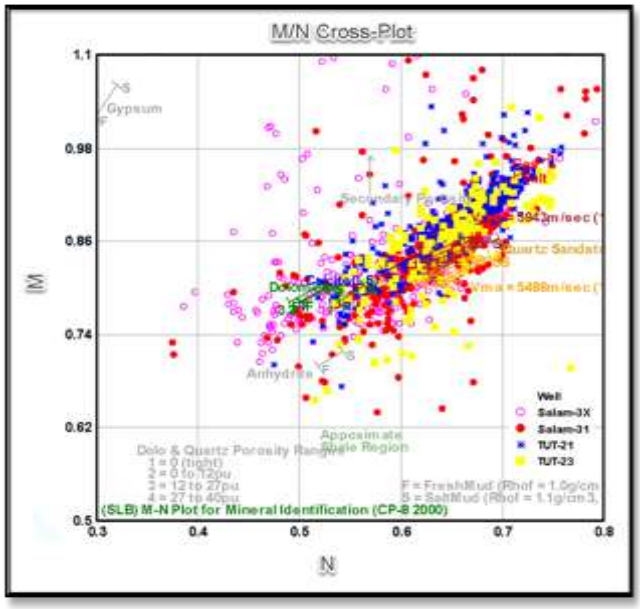

Fig. (7): M-N cross-plot for Upper Safa Reservoir in TUT-21, TUT-23, Salam-3X and Salam-31wells

Petrophysical Evaluation

Vertical Litho-Saturation Cross-plots

The variance in lithological vertical distribution can be seen in cross-plots of litho-saturation, effective porosity, resistivity (Rd, Rs and MSFL), and coefficients of fluid saturations such as hydrocarbon and water saturations for the studied formation against depth.

Analysis of the cross-plots indicates that the Lower Safa Member consists primarily of sandstone as the main lithological component, with shale intercalation and calcareous cement, together with the presence of a few beds of limestone **(Fig. 8)**. Dolomite and limestone disappear in the salam-3X and TUT-55 wells. There are a few streaks of coal in TUT-55 well only. Additionally, it demonstrates that the main lithological component of the Upper Safa Member is shale with minor siltstone intercalation, together with sandstone bodies and calcareous cement, with few beds of limestone. There are also some streaks of coal **(Fig. 9).**

The hydrocarbon potentiality is performed by evaluating the vertical and horizontal distribution of the petrophysical results. **Table (1)** displays values for reservoir parameters calculated by averaging various log parameters.

Table (1): Well Log Parameters of the Jurassic Lower & Upper Safa Reservoirs, Shoushan Basin

Well Name	Formation	Total Thickness (FT)	Φ_e (%)	V_{sh} (%)	Gross Sand (FT)	Net Pay (FT)	N/G (%)	Sxo (%)	Sw (%)	Sh (%)	Shr (%)	Shm (%)
Salam-3X	Upper Safa	670.5	10.6	9.5	92.5	81.5	88.1	90.8	18.4	81.6	9.2	72.4
Salam-31		679	12.3	10.1	93	59.5	64.0	93.4	12.2	87.8	6.6	81.2
TUT-21		794	10.9	4.4	138	136.5	98.9	91.1	12.6	87.4	8.9	78.5
TUT-23		728	10.3	7.7	33	33	1.00	96.4	20.1	79.9	3.6	76.3
TUT-55		767	10	6.1	122.25	79.25	64.8	95.1	20.6	79.4	4.9	74.5
Salam-3X	Lower Safa	193.5	21.4	17.2	118.25	37.75	31.9	79.8	32.3	67.7	20.2	47.4
Salam-31		214	11.1	1.5	141	3.5	2.50	96.3	33.1	66.9	3.7	63.2
TUT-21		139	11.1	7.3	37.5	35	93.3	88.0	12.2	87.8	12	75.8
TUT-23		185	10	7.5	81	54.5	67.3	80.7	20.2	79.8	19.3	60.5
TUT-55		111	13.7	3.8	42.25	3.5	8.30	93.2	29.1	70.9	6.8	64.1

Total Thickness (FT): the thickness of member

Φ_e%= effective porosity

V_{sh}%= shale volume

Sxo%= saturation of invaded zone

Sw%= water saturation

Sh%= hydrocarbon saturation

Shr%= residual hydrocarbon saturation

Shm%= movable hydrocarbon saturation

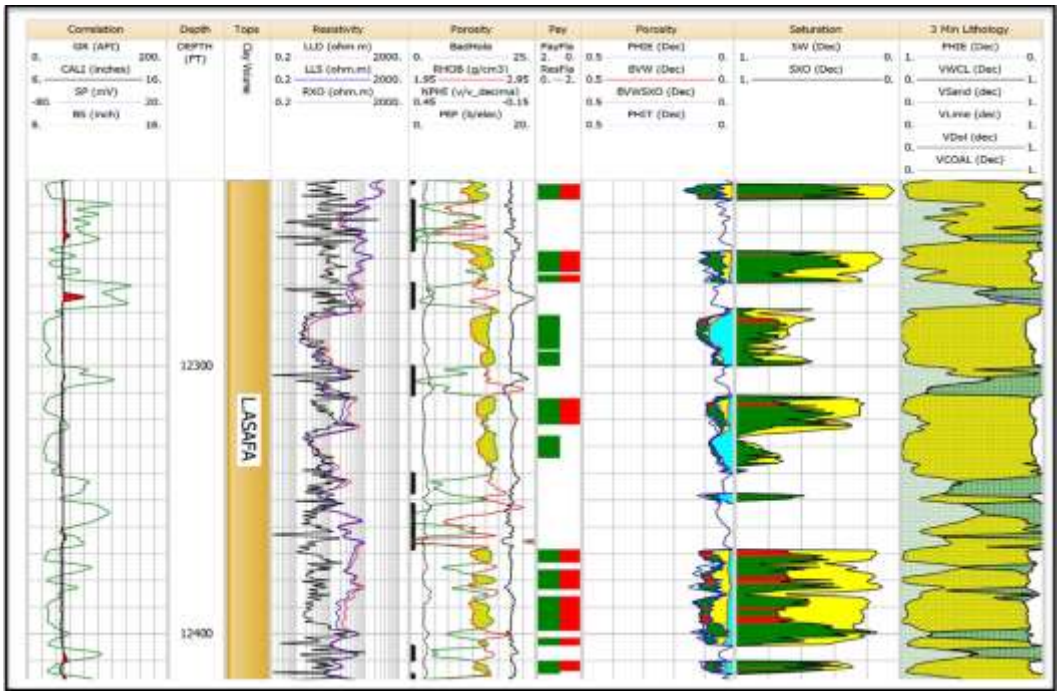

Fig. (8): Representative Litho-saturation cross-plot of the Lower Safa reservoir in TUT-23 well

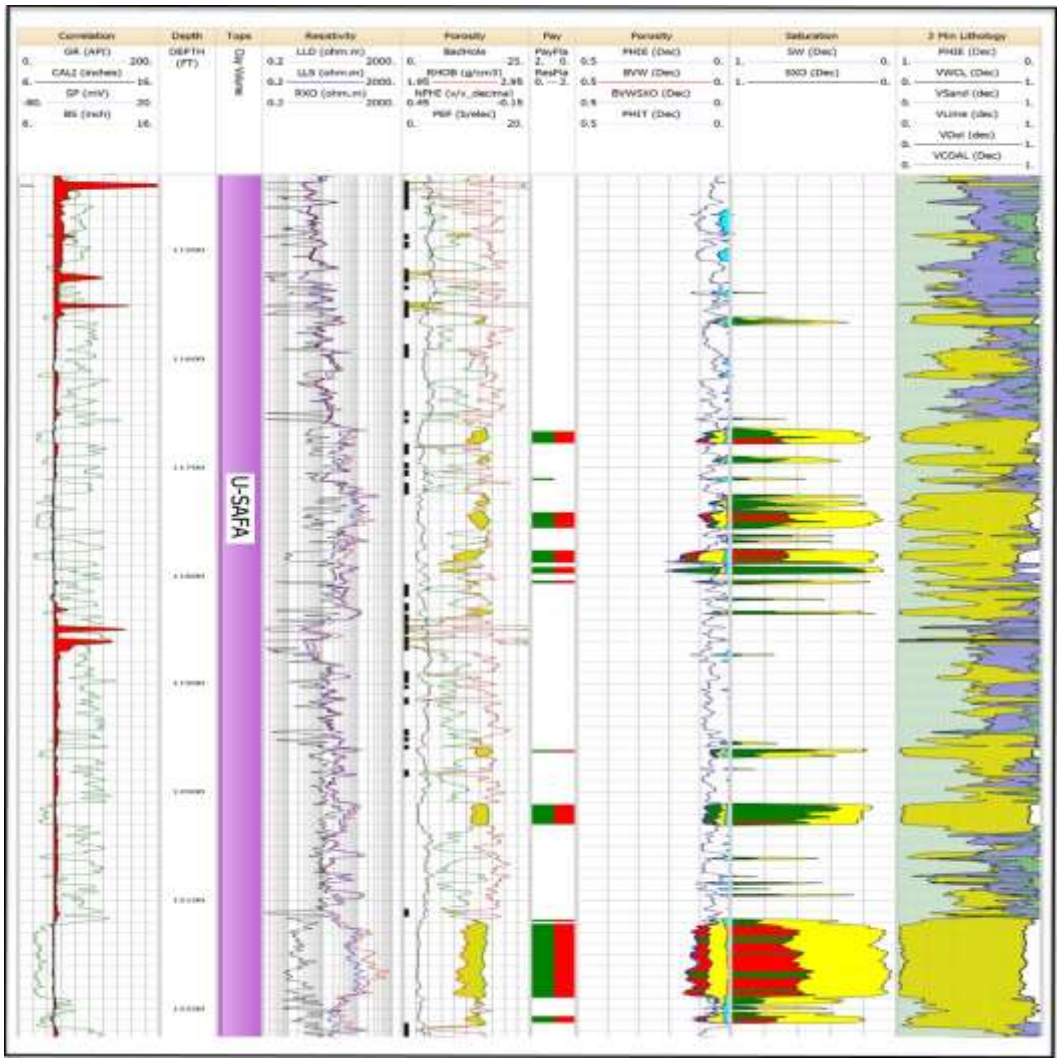

Fig. (9): Representative Litho-saturation cross-plot of the Upper Safa reservoir in TUT-21 well

Reservoir Mapping

The contour maps of the log-derived petrophysical parameters illustrate their overall distribution throughout the Lower Safa reservoir (**Figs 10-13**). The effective porosity value increases toward the southeastern direction and decreases toward the northwestern direction. The maximum effective porosity value of 21.4% is at Salam-3X well (**Fig. 10**). The shale volume content increases toward the southeastern direction and decreases toward the eastern and southeastern directions (**Fig. 11**). The net pay distribution map (**Fig. 12**) shows an increase toward the northwestern direction at TUT-23 and decreases toward the southeastern and central parts directions of the study area. The hydrocarbon saturation increases in the northeastern direction and decreases in the southeastern direction. The hydrocarbon saturation reaches its maximum value of 87.8% at TUT-21 (**Fig. 13**).

Similarly, the log-derived petrophysical parameters throughout the Upper Safa reservoir are displayed in contour maps to display their general distribution. The effective porosity value increases toward the southeastern direction and decreases towards the central part direction to reach its minimum value at TUT-55. The maximum effective porosity is found at Salam-31 well (**Fig. 14**). The shale volume content increases toward the southeastern and decreases toward northeast (**Fig. 15**). As may be seen from the net pay distribution map, the net pay increases toward the northeast direction at TUT-21 well and decreases toward the northwestern (**Fig. 16**). The hydrocarbon saturation increases toward the southeastern, and decreases toward the central part and northwestern directions. The hydrocarbon saturation reaches its maximum value of 87.8% at Salam-31 well (**Fig**. **17**).

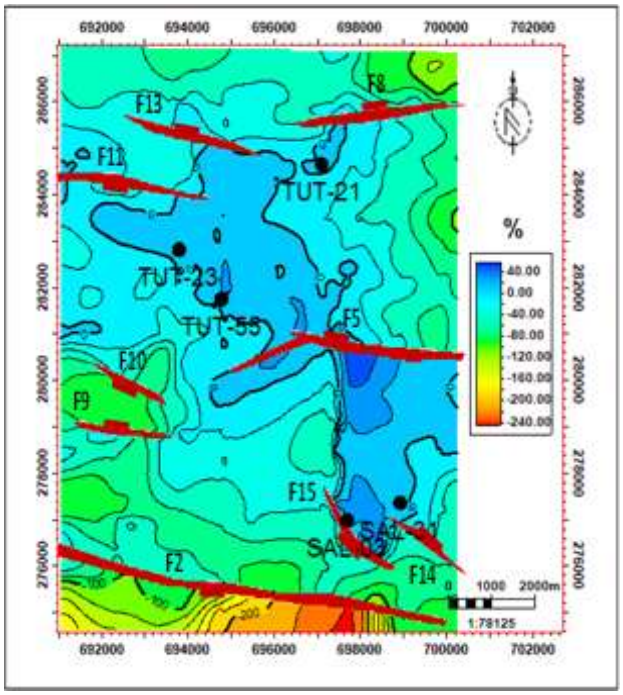

Fig. (10): Effective porosity map of the Lower Safa reservoir.

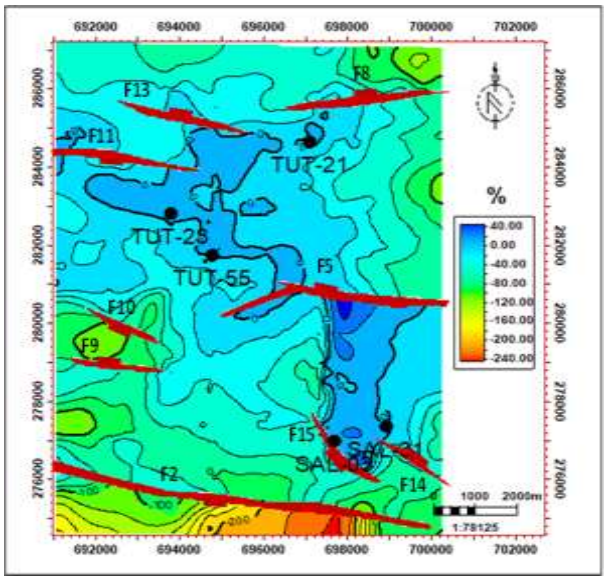

Fig. (11): Shale volume map of the Lower Safa reservoir.

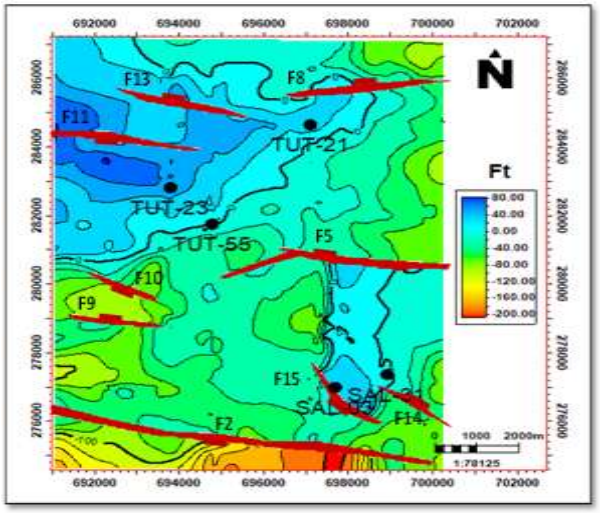

Fig. (12): Net pay thickness map of the Lower Safa reservoir.

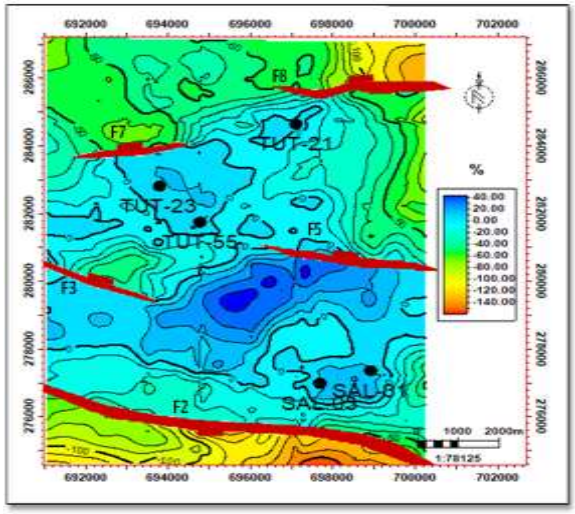

Fig. (15): Shale volume map of the Upper Safa reservoir.

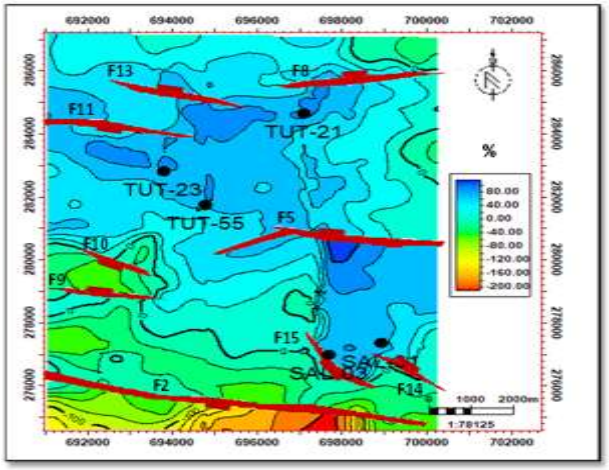

Fig. (13): Hydrocarbon saturation map of the Lower Safa reservoir.

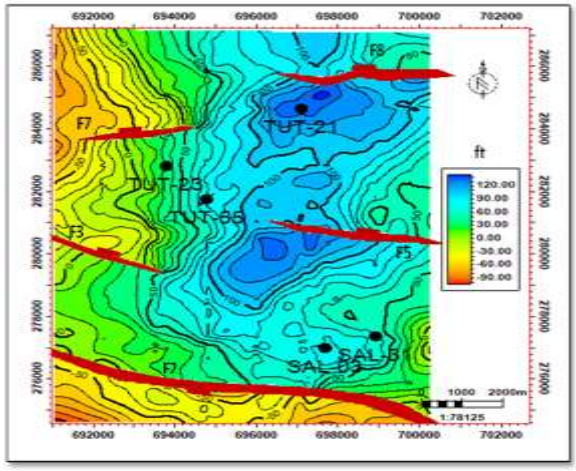

Fig. (16): Net pay thickness map of the Upper Safa reservoir.

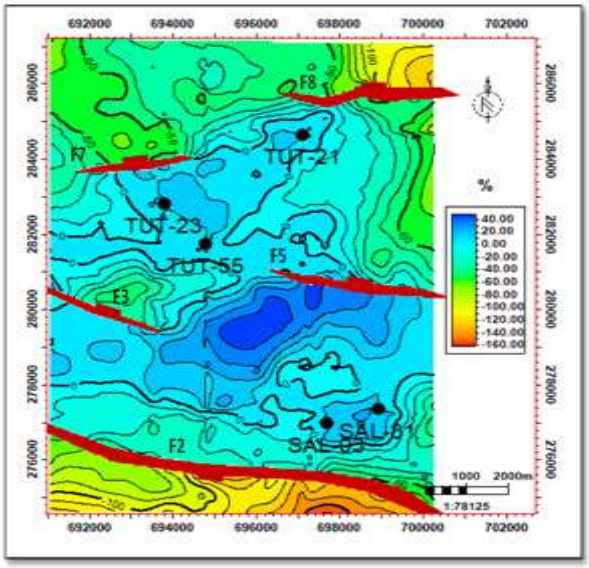

Fig. (14): Effective porosity map of the Upper Safa reservoir.

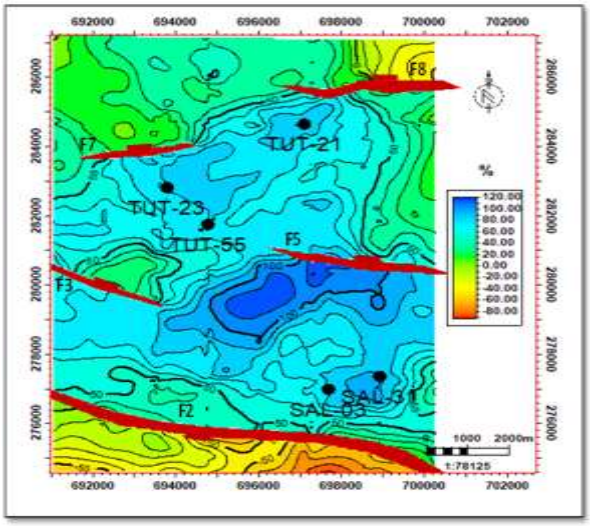

Fig. (17): Hydrocarbon saturation map of the Upper Safa reservoir.

Conclusion

The petrophysical characteristics of the Lower and Upper Safa members show that, the shale content (VSH) for the lower Safa increases towards the southeastern and northwestern directions where it achieves the upper limit value (17.2%) at Salam-3X, and falls towards the southeastern direction to reach (1.5%) as a lower limit value at Salam-31 well, while the shale content of the Upper Safa increases towards the southeastern direction where it achieves the upper limit value (10.1%) at Salam-31, and falls towards the northeastern direction to reach (4.4%) as a lower limit value at TUT-21 well.

The effective porosity (Φeff) for the Lower Safa is increasing towards the southeastern direction where it reaches (21.4%) at Salam-3X well, while it falls towards the northwestern direction to reach (10%) as a lower limit value at TUT-23 well. On the other hand, the Upper Safa is increasing towards the southeastern direction where it reaches (12.3%) at Salam-31 well it falls towards the central part direction to reach (10%) as a lower limit value at TUT-55 well.

The hydrocarbon saturation (Shr) for the Lower Safa is decreasing towards the southeast direction where it passes the minimum value (66.9%) at Salam-31 well and for the Upper Safa is decreasing towards the central part direction where it passes the minimum value (79.4%) at TUT-55 well. The increasing is observed towards the northeast direction where the upper limit value was (87.8%) at TUT-21 well for the Lower Safa, while it is observed towards the south eastern direction where the upper limit value was (87.8%) at Salam-31 well for the Upper Safa.

Moving hydrocarbon is the most significant parameter, according to vertical litho-saturation crossplots of petrophysical parameters that identify the most effective sand zones. According to the hydrocarbon distribution maps, the Lower and Upper Safa reservoirs both exhibit a general increase in the northeastern and southeastern regions.

The density-neutron and M-N cross-plots of the Lower and Upper Safa reservoirs demonstrate that the predominant lithology is sandstone with some calcareous cement and sporadic weak signs of natural gas impact.

These areas are thought to be the most promising ones for further investigation and reservoir development.

Acknowledgements

The Egyptian General Petroleum Corporation (EGPC), Cairo, Egypt, officials kindly granted the authors permission to collect the well-log data utilized in this work, Khalda Petroleum

Company in Cairo for contributing the well-log data used in this work. Two anonymous reviewers are thanked for their critical review and constructed comments that improved the MS.

References

Abdel-Fattah, Th.A. (2017): Source rock evaluation of the pre-Aptian section at some wells, Matruh sub-basin, northern western Desert Egypt. In: Schandelmeier, H. and Thorweihe, Ulf (Eds.): Geoscientific Research in Northeast Africa 1st Edition, CRC Press, pp. 391-393.

Abdel-Fattah, Th.A. ; Rashed, M.A. and Diab, A.I. (2019): Reservoir compartmentalization phenomenon for lower safa reservoir, obaiyed gas field, North Western Desert, Egypt. *Arab. J. Geosci.*, Springer Berlin Heidelberg, 12: 1-13.

Abu Shady, A.N. (1998): Sedimentary environments and hydrocarbon potentialities of the Kharita Formation Lower Cretaceous, central part of Abu Gharadig basin, Western Desert, Egypt. M.Sc. Thesis. Tanta Univ., Egypt, 128 P.

Amin, M.S. (1961): Subsurface features and oil prospects of the Western Desert, Egypt. In: Proceeding of the 3rd Arab. Petro. Cong., Alexandria, Egypt, V. 2: 8 p.

Badawy, M.; Abdel Fattah, Th.A.; Abou Shagar, S.; Diab, A.I.; Rashed, M.A. and Osman, M. (2023): Identifying the hydrocarbon potential from seismic, geochemical, and wireline data of the Sallum intra-basin, North Western Desert of Egypt. *NRIAG-JAG, Taylor & Francis,*12: 1-18.

Dolson, J.C.; Shann, M.V.; Matbouly, S.; Harwood, C.; Rashed, R. and Hammouda, H. (2001): The petroleum potential of Egypt. In: Downey, M.W., Threet, J.C., Morgan, W.A. (Eds.), Petroleum Provinces of the Twenty-first Century: *AAPG, Tulsa, Oklahoma,*74: 453 – 482.

EGPC (Egyptian General Petroleum Corporation) (1992): Western Desert, oil and gas fields, a comprehensive overview. EGPC 11th Petrol. Expl. and Prod. Conf., Cairo, 431 p.

EGPC (Egyptian General Petroleum Corporation) (1998): Western Desert oil and gas fields, A comprehensive overview. EGPC 14th Petrol. Conf., Cairo, 2: 422-444.

El Awady, M.M.; Abdel Hameed, A.T.; Hassan, A.A. and Abu Shady, A.N. (1998): Depositional Environments from Natural Gamma Rays Spectrometry, Abu Gharadig Basin, North Western Desert, Egypt. 1st International Symposium on geophysics, Tanta Univ., pp. 358 – 366.

El-Dakak, M.A.; Abdelfattah, Th.A.; Diab, A.I.; Kassem, M.A. and Knapp, C.C. (2021): Integration of borehole depth imaging and seismic reflection results in reservoir delineation: An example from The Alam El Bueib 3C field, Northern Western Desert, *Egypt. J. Afr. Earth Sci., Elsevier,* 184, article id. 104322

El-khadragy, A.A. and Sharaf, M. (1994): Inferring the basement structure of North Western Desert, using potential field data. Bull. *Fac. Sci., Zagazig Univ.*, 16 (2): 92 – 110.

El-khadragy, A.A.; Saad, M.H. and Azab, A. (2010): Crustal modeling of south Sitra area, North Western Desert,

Egypt, using Bouguer gravity data. *J. Appl. Sci. Res.*, 61(1): 22 – 27.

Eysa, E.A. (2016): Petrophysical Evaluation of Middle Jurassic Reservoirs, Shams Oil Field, North Western Desert, Egypt. *IOSR J. App. Geol. Geophy*. (IOSR-JAGG), 4 (1): 58-68.

Keeley, M.L.; Dungworth, G.; Floyd, C. S.; Forbes, G. A.; King, C.; McGarva, R. M. and Shaw, D. (1990): The Jurassic System in northern Egypt: I. Regional stratigraphy and implications for hydrocarbon prospectivity. *J. Petro. Geol. (JPG)*, 13: 397–420

Khalda Petroleum Company (2010): Internal Unpublished report.

Meshref, W.M. (1982): Regional Structural Setting of Northern Egypt. EGPC 6th Explo. Conf., Cairo, Egypt, 1: 17 – 34.

Osman, W.M.; Abd El-Gawad, .A; Mesbah, M.A. and Abd El-Fattah, Th.A. (2017): Application of well logging and Seismic techniques for Evaluation of Hydrocarbon Potentialities, East Abu Sennan Area, Western Desert, Egypt. *Int. J. Sci. Eng. Appl. Sci. (IJSEAS)*, 3: 2395-3470.

Saad, A.; Abdel Fattah, Th.; Holial H.; Diab, A.I. and Abou Shagar, S. (2023): Exploration of new hydrocarbon leads in the eastern flank of Abu Gharadig Basin, North Western Desert, Egypt. *Alexandria Engin. J.*, 66: 669-690

Said, R. (1962): The geology of Egypt. Elsevier Publishing Co., Amsterdam New York, 377 P.

Shalaby, M. R.; ElAwady, M. M.; Abdel Hameed, A.T. and Abu Shady, A.N. (2000): Structural Setting and Sedimentary Environments Using Dipmeter Analysis of Some Jurassic Reservoirs, North Western Desert, Egypt. 5th International Conf. of Geology of the Arab World (GAW-5), Cairo Univ., Egypt, PP. 217 – 220.

Shalaby, M.R.; Hakimi, M.H. and Abdullah, W.H. (2013): Petroleum system analysis of the Khatatba Formation in the Shoushan Basin, north Western Desert, Egypt. *Arab J. Geosci*.,7 (10): 20 P.

Sultan, N. and Abd El-Halim, M. A. (1988): Tectonic framework of northern Western Desert, Egypt, and its effect on hydrocarbon accumulations: Egyptian General Petroleum Corporation 9th Exploration and Production Conference, Cairo, Egypt, November 20–23, 1–23.

Zein El-Din, M.Y.; Abd El-Gawad, E.A.; El-Shayb, H.M. and Haddad, I.A. (2001): Geological studies and hydrocarbon potentialities of the Mesozoic rocks in Ras Kanayis onshore area, north Western Desert, *Egypt. Ann. Geol. Surv. Egypt*, XXIV: 115–134.

خصائص الخزان لمتكون الصفا الجوراسي ، حوض شوشان ، شمال الصحراء الغربية ، مصر

مى الغندور [١]، عبدالمنعم أبوشادى [٢] ، عبدالعزيز عبدالدايم [١] ، على سليمان [١]

١- قسم الجيولوجيا - كلية علوم - جامعة طنطا
٢- شركه بترونفرتيتي للبترول – المعادى – القاهرة – مصر

تقيم هذه الدراسة الخصائص الصخرية والبتروفيزيائية لخزانات الصفا الجوراسي في الجزء الغربي من حوض شوشان، شمال الصحراء الغربية لمصر. تم استخدام السجلات البئرية لخمسة آبار من حقلى TUT و Salam لتقييم المعايير البتروفيزيائية المختلفة. تم استخدام المخططات التبادلية للسجلات البئرية الكثافة / النيوترون (D/N) ثنائية المسامية وثلاثية المسامية (M-N) لتحديد الصخر ومسامية الخزانات المدروسة. وفقًا لنتائج التشبع الصخري المتقاطع ، يتكون عضو الصفا السفلي بشكل أساسي من الحجر الرملي ، مع عدد قليل من الطبقات البينية من الحجر الجيري ، والتقطيع الصخري الطفلى، والأسمنت الجيري ، بينما يتكون عضو الصفا العلوي بشكل أساسي من الصخر الطفلى ، مع بضعة طبقات من الحجر الجيري وأجسام الحجر الرملي. يظهر تأثير الغاز الطبيعي في بعض مخططات D/N المتقاطعة في كلا العضوين. استخدم التخطيط الرأسى للمعاملات البتروفيزيائية المشتقة من التشبع الصخري لتحديد مناطق الرمل الأكثر فعالية لكل بئر. يزداد على الهيدروكربون المتحرك في الغالب في الأجزاء العلوية والمتوسطة من خزان الصفا السفلي وفي الأجزاء الوسطى والسفلى من خزان الصفا العلوي. تُظهر خرائط التوزيع المُنشأة لخزانى الصفا السفلى والعلوى أن الجزأين الشمالي والجنوبي الشرقي، على التوالي من الحقلين المدروسين هما أكثر المناطق الواعدة للتطوير المستقبلي.